JOURNAL OF VIROLOGY, May 2003, p. 5286–5294 Vol. 77, No. 9
0022-538X/03/$08.00+0 DOI: 10.1128/JVI.77.9.5286–5294.2003

Rapid Tumor Formation of Human T-Cell Leukemia Virus Type 1-Infected Cell Lines in Novel NOD-SCID/γc^{null} Mice: Suppression by an Inhibitor against NF-κB

M. Zahidunnabi Dewan,[1] Kazuo Terashima,[1] Midori Taruishi,[1] Hideki Hasegawa,[2] Mamoru Ito,[3] Yuetsu Tanaka,[4] Naoki Mori,[5] Tetsutaro Sata,[2] Yoshio Koyanagi,[6] Michiyuki Maeda,[7] Yoko Kubuki,[8] Akihiko Okayama,[8] Masahiro Fujii,[9] and Naoki Yamamoto[1]*

Department of Molecular Virology, Bio-Response, Graduate School, Tokyo Medical and Dental University, Tokyo 113-8519,[1] Department of Pathology, National Institute of Infectious Diseases, Tokyo 162-8640,[2] Central Institute for Experimental Animals, Kawasaki 216,[3] Department of Infectious Disease and Immunology, Okinawa-Asia Research Center of Medical Science,[4] and Department of Virology,[5] Faculty of Medicine, University of the Ryukyus, Okinawa 905-0215, Department of Virology, School of Medicine, Tohoku University, Sendai 980-8575,[6] Institute for Frontier Medical Sciences, Kyoto University, Kyoto 606-8507,[7] Department of Internal Medicine II, Miyazaki Medical College, Miyazaki 889-1601,[8] and Department of Virology, Niigata University School of Medicine, Niigata 951,[9] Japan

Received 16 August 2002/Accepted 24 January 2003

We established a novel experimental model for human T-cell leukemia virus type 1 (HTLV-1)-induced tumor using NOD-SCID/γc^{null} (NOG) mice. This model is very useful for investigating the mechanism of tumorigenesis and malignant cell growth of adult T-cell leukemia (ATL)/lymphoma, which still remains unclear. Nine HTLV-1-infected cell lines were inoculated subcutaneously in the postauricular region of NOG mice. As early as 2 to 3 weeks after inoculation, seven cell lines produced a visible tumor while two transformed cell lines failed to do so. Five of seven lines produced a progressively growing large tumor with leukemic infiltration of the cells in various organs that eventually killed the animals. Leukemic cell lines formed soft tumors, whereas some transformed cell lines developed into hemorrhagic hard tumors in NOG mice. One of the leukemic cell lines, ED-40515(−), was unable to produce visible tumors in NOD-SCID mice with a common γ-chain after 2 weeks. In vivo NF-κB DNA binding activity of the ED-40515(−) cell line was higher and the NF-κB components were changed compared to cells in vitro. Bay 11-7082, a specific and effective NF-κB inhibitor, prevented tumor growth at the sites of the primary region and leukemic infiltration in various organs of NOG mice. This in vivo model of ATL could provide a novel system for use in clarifying the mechanism of growth of HTLV-1-infected cells as well as for the development of new drugs against ATL.

Human T-cell leukemia virus type-1 (HTLV-1) induces adult T-cell leukemia/lymphoma (ATL/L), a fatal lymphoproliferative disorder, and HTLV-1-associated myelopathy/tropical spastic paraparesis, a chronic progressive disease of the central nervous system after a long period of latent infection (12, 33, 48). This long latency suggests that multiple genetic events, which accumulate in HTLV-1-infected cells, are involved in the development of ATL. HTLV-1 transforms primary human T-cells in vitro and a unique viral gene Tax is considered to play a central role in HTLV-1-induced transformation. However, HTLV-1-infected cell lines derived from a leukemic cell clone failed to express significant amounts of Tax and other viral proteins, suggesting that the expression of viral proteins is not always necessary for leukemic proliferation at the late stage of the disease. On the other hand, the observation that NF-κB, which is strongly induced by Tax, is indispensable for the maintenance of the malignant phenotype of HTLV-1 provides a possible molecular target for ATL therapy (23, 39) as well as the treatment of some cancers (1, 14, 40). In resting cells, binding to inhibitory IκBs retains NF-κB in the cytoplasm in an inactive form. On stimulation, IκBs are rapidly phosphorylated, ubiquitinated, and degraded by a proteosome-dependent pathway allowing active NF-κB to translocate into the nucleus where it can activate the expression of a number of genes (2). Like HTLV-1-infected cells in vitro, leukemic cells from ATL patients in vivo display a constitutive NF-κB binding activity and increased degradation of IκBα (28). However, the precise molecular mechanism of tumorigenesis and the development of ATL after HTLV-1 infection remain obscure.

The severe combined immunodeficient (SCID) mice lacking functional T and B cells (4, 27) were engrafted successfully with human hematopoietic or neoplastic cells (6, 13, 17, 20, 21, 30, 34, 35, 44). SCID mice also have been utilized in a study on the mechanism and therapeutic strategy of ATL. Indeed, it has been reported that HTLV-1-infected cell lines derived from a leukemic clone produced tumors during a 2- to 4-month follow-up period but in vitro-transformed cell lines expressing Tax and other viral antigens failed to do so in SCID mice even at 6 months after inoculation (10, 16). However, two major drawbacks, namely, the long period of time required for tumor formation and the limitation of its use to certain cell lines, appear to hinder wider use of this animal model. To overcome

* Corresponding author. Mailing address: Department of Molecular Virology, Bio-Response, Graduate School, Tokyo Medical and Dental University, 1-5-45 Yushima, Bunkyo-ku, Tokyo 113-8519, Japan. Phone: 81-3-5803-5178. Fax: 81-3-5803-0124. E-mail: yamamoto.mmb@tmd.ac.jp.

these problems we have developed a new SCID mouse strain, the NOG mouse, which is a special type of animal that has immunological multifunctional defects in NK activity, macrophage function, complement activity and function of dendritic cells (18). HTLV-1-infected cell lines were inoculated subcutaneously in the postauricular region of NOG mice enabling macroscopic observation in the study of the mechanism of tumorigenesis and malignant growth of ATL and the development of new drugs against ATL.

There is no effective treatment for ATL patients. ATL still has a poor prognosis mainly because of its resistance to conventional as well as high-dose chemotherapy. Bay 11-7082 is a selective inhibitor of tumor necrosis factor alpha-induced phosphorylation of IκBα without affecting the constitutive activation of IκBα phosphorylation, resulting in decreased NF-κB and decreased expression of adhesion molecules (31). Very recently, we reported that Bay 11-7082 specifically inhibited nuclear translocation of NF-κB and caused selective apoptosis of HTLV-1-infected cell lines and primary ATL cells in vitro (29). In addition, this compound is also known to induce apoptosis of lymphoma cells from patients with primary effusion lymphoma or cutaneous T-cell lymphoma in vitro (19, 22).

We show here that a progressively growing large tumor was rapidly and reproducibly induced in mice inoculated with HTLV-1-infected cell lines derived from both leukemic and transformed cell clones only within 2 weeks. We also examined in vivo tumor growth of an HTLV-1-infected cell line between NOG and NOD-SCID mice to address the role of the common γ-chain. We also provide evidence that the NF-κB-inhibitory effect of Bay 11-7082 is linked to regression of the tumor and that the drug prevented leukemic infiltration of tumor cells in various organs of NOG mice. These results suggest that the NOG mouse model of HTLV-1-infected cell lines would be useful for investigating the in vivo molecular pathogenesis of diseases, infiltration into different organs and therapeutic measures for ATL patients.

MATERIALS AND METHODS

Mice. NOG and NOD-SCID mice were obtained from the Central Institute for Experimental Animals (Kawasaki, Japan). All mice were bred and maintained under specific-pathogen-free conditions in the Animal Center of National Institute of Infectious Diseases (Tokyo, Japan). The Ethical Review Committee of the Institute approved the experimental protocol.

Cell lines. ED-40515(−), MT-1, and TL-Oml are interleukin-2 (IL-2)-independent and Tax nonexpressing human T-cell lines of leukemic cell origin established from ATL patients. SLB-1, Hut-102, MT-2, MT-4, M8116, and TY8-3/MT-2 are IL-2-independent and Tax expressing HTLV-1-infected transformed T-cell lines, and Jurkat is an HTLV-1-negative T-cell line. These cell lines were cultured in RPMI 1640 medium (Nikken Bio-laboratory, Kyoto, Japan) with 10% heat-inactivated fetal bovine serum (JRH Biosciences, Lenexa, Kans.), 2 mM L-glutamine, 100 U of penicillin per ml, and 100 μg of streptomycin per ml at 37°C and 5% CO_2.

Inoculation of cell lines into SCID mice. Cells were washed twice with serum-free RPMI 1640 medium. These cells were resuspended in serum-free RPMI 1640 medium. Mice were anesthetized with ether and cells were inoculated subcutaneously in the postauricular region of SCID mice at a dose of 1 to 7.5 × 10^7 cells per mouse.

Growth measurement of subcutaneous tumor and dispersion of cells. Mice were sacrificed during the 2- to 3-week follow-up period after inoculation with different cell lines. The subcutaneous tumor was excised from the postauricular region of SCID mice. We measured the length, width, and height of the tumor by the Somers scale. Tumor tissues obtained from mice inoculated with the ED-40515(−) cell line after 1 week and 2 weeks for measuring the growth curve in both strains of mice. Next, the tumor tissues were incubated and digested by shaking in RPMI 1640 plus 10% fetal calf serum containing collagenase (1 mg/ml; Seikagaku Kogyo, Tokyo, Japan) plus DNase type I (0.5 mg/ml; Sigma) at 37°C for 30 min. Dispersed cells were collected and the same procedure was conducted as described above. All dispersed cells were filtered with a 40-μm-pore-size filter and washed twice with serum-free medium at 400 × *g* for 5 min. The supernatant was aspirated and the cell pellets were collected. Number of cells was counted by the trypan blue method.

Histological and cytological examination. After sacrificing the mice, tumor tissues, peripheral blood, and various organs were collected. Part of the excised tumor tissues were fixed with dry-ice acetone and embedded in Tissue-Tek OCT compound (Sakura Finetechnical Co. Ltd., Tokyo, Japan) and stored at −80°C before use. Frozen sections of the tumor tissues were prepared by Cryostat and fixed in acetone at room temperature for 20 min. The remaining tumor tissues and organs were fixed with 4% paraformaldehyde for hematoxylin and eosin (H&E) staining and examined under a microscope. Blood was collected from the heart of mice with heparinized syringes. Peripheral blood mononuclear cells (PBMNCs) were isolated from the blood by density gradient concentration with Ficoll-Hypaque. Cytospin specimens of in vitro culture cells and PBMNCs were prepared and fixed in methyl alcohol for May-Grunwald and Giemsa staining and fixed in acetone for immunostaining. For immunostaining, frozen sections of tumor tissues and cytospin samples of in vitro culture cells were incubated with a 1:50 dilution of primary antibody against human cells, anti-CD4 (Novocastra Laboratory. Ltd.), anti-CD25 (Kamiya Biomedical Company, Seattle, Wash.), anti-CD3, and anti-CD8 mouse (DAKO A/S), anti-Tax (MI-73) and anti-Gag (GIN-14) mouse monoclonal antibodies. This was followed by washing in phosphate-buffered saline (PBS) and then incubation with horseradish peroxidase-conjugated rabbit anti-mouse immunoglobulin G antibody (1:200) and washed in PBS. Positive staining was visualized after incubation of these samples with a mixture of 0.05% 3,3′-diaminobenzidine tetrahydrochloride in 50 mM Tris-HCl buffer and 0.01% hydrogen peroxide for 5 to 10 min. The samples were counterstained with methyl green for 15 min, hydrated completely, cleaned in xylene, and then mounted.

Western blotting. Culture cells and cells from tumors were lysed by a low-salt lysis buffer (10 mM Tris-HCl [pH 8.0], 140 mM NaCl, 3 mM $MgCl_2$, 1 mM phenylmethylsulfonyl fluoride [PMSF], and 0.5% Nonidet) on ice for 30 min, followed by centrifugation at 14,000 rpm for 10 min at 4°C. The cell lysates were mixed with an equal volume of twofold-concentrated sample buffer with 2-mercaptoethanol and treated for 5 min at 100°C. Equal amounts (25 μg) of protein from the cell lysates were electrophoresed on sodium dodecyl sulfate–10% polyacrylamide gel and transferred to a Clear Blot Membrane-p (ATTO, Tokyo, Japan) by an electric Western blotting system. The membranes were washed with PBS-Tween (0.1%) and blocked in PBS containing 3% skim milk overnight at 4°C. The membranes were incubated with 1 μg per ml of primary antibody, anti-Tax monoclonal antibody (MI-73) followed by washing in PBS-Tween (0.1%) and incubated again with horseradish peroxidase-conjugated rabbit anti-mouse immunoglobulin G (1:3,000). Protein bands were visualized by an enhanced chemiluminescence substrate and the FLA-2000 system (Fuji Photo Film Co. Tokyo, Japan).

Preparation of nuclear extracts. Cells (3 × 10^6) were washed twice with cold PBS and the cell pellet was resuspended in 200 μl of hypotonic buffer A (HEPES, 10 mmol/liter, pH 7.9; KCl, 10 mmol/liter; EDTA, 0.15 mmol/liter; EGTA, 0.15 mmol/liter; PMSF, 0.1 mmol/liter; leupeptin, 100 μg/liter; aprotinin, 100 μg/liter) including 1% Nonidet and incubated on ice for 15 min. Cell suspensions were vortexed briefly and microcentrifuged at 14,000 rpm for 5 min at 4°C. The supernatants were removed, and the cell pellets were suspended in 200 μl of isotonic B buffer (HEPES, 20 mmol/liter, pH 7.8; NaCl, 100 mmol/liter; EDTA, 0.1 mmol/liter; 25% glycerol), vortexed briefly and microcentrifuged at 14,000 rpm for 3 min at 4°C. Thereafter, the cell pellets were resuspended in 100 μl of hypertonic C buffer (HEPES, 20 mmol/liter, pH 7.8; NaCl, 400 mmol/liter; EDTA, 0.1 mmol/liter; 25% glycerol; PMSF, 0.1 mmol/liter; leupeptin, 100 μg/liter; aprotinin, 100 μg/liter; DTT, 10 mmol/liter) including 1 M NaCl, inoculated at 4°C for 30 min with continuous high speed shaking and microcentrifuged at 14,000 rpm for 3 min. The supernatants were collected, the protein concentrations measured by the method of Bradford and the supernatants stored at −80°C for use.

Electrophoresis mobility shift assay (EMSA). As previously described, nuclear extracts (5 μg of protein) were incubated in 12 μl of binding buffer (HEPES, 10 mmol/liter, pH 7.8; NaCl, 100 mmol/liter; EDTA 1 mmol/liter; 25% glycerol), 1 μg of poly [d(I-C)] and ^{32}P-labeled κB probe derived from the H-2K promoter (22a) for 30 min at room temperature. To identify the subunits constituting the NF-κB complexes, specific antibodies against p50, p65, and c-Rel (Santa Cruz Biotechnology, Santa Cruz, Calif.) were used. Antibodies was added to the nuclear extract, and the mixture was allowed to stand for 30 min at room

TABLE 1. In vitro and in vivo characteristics of HTLV-1-infected cell lines

Cell line	Origin[a]	In vitro characteristics		No. of cells inoculated/mouse (10^7)[c]	In vivo characteristics			
		Proliferation pattern	Tax[b]		Inoculation route[d]	No. of mice with visible tumor/no. of mice inoculated[e]	Day of sacrifice	Average size of tumor (mm)[f]
ED-40515(−)	L	Dispersed	−	1	s.c.	37/37	15	25 × 20 × 12
				7.5	i.m.	1/1	15	23 × 18 × 12
SLB-1	IT	Clustered	+	1	s.c.	15/15	15	19 × 10 × 16
				7.5	i.m.	1/1	15	20 × 10 × 15
MT-1	L	Dispersed	−	1	s.c.	7/7	22	22 × 15 × 10
				7.5	i.m.	1/1	20	21 × 14 × 10
TL-oml	L	Dispersed	−	1	s.c.	7/7	22	23 × 15 × 10
				7.5	i.m.	1/1	20	18 × 15 × 10
Hut-102	IT	Clustered	+	1	s.c.	4/4	22	21 × 13 × 16
				7.5	i.m.	1/1	20	10 × 10 × 7
MT-2	IT	Clustered	+	7.5	s.c.	1/1	20	10 × 9 × 8
				7.5	i.m.	1/1	20	9 × 10 × 7
MT-4	IT	Clustered	+	7.5	s.c.	1/1	20	5 × 5 × 4
				7.5	i.m.	1/1	20	5 × 4 × 3
M8116	IT	Clustered	+	7.5	s.c.	0/1	20	Sesame
				7.5	i.m.	0/1	20	Sesame
TY8-3/MT-2	IT	Clustered	+	7.5	s.c.	0/1	20	Sesame
				7.5	i.m.	0/1	20	Sesame

[a] L, leukemic; IT, in vitro transformed.
[b] −, negative; +, positive.
[c] Mice were injected with 1×10^7 to 7.5×10^7 cells per mouse.
[d] s.c., subcutaneous; i.m., intramuscular.
[e] Number of animals in which visible tumor developed.
[f] Average tumor size of individual mouse was measured as described in Materials and Methods and is given here as length × width × height.

temperature before incubation with the radiolabeled probe. DNA-protein complexes were analyzed by electrophoresis in 5% polyacrylamide gel in 0.5× TBE (Tris, 44.5 mmol/liter; boric acid, 44.5 mmol/liter; EDTA, 1 mmol/liter). After electrophoresis, the gels were dried and subjected to autoradiography.

Administration of Bay 11-7082. Bay 11-7082 was obtained from the Calbiochem-Novabiochem Corporation, La Jolla, Calif. The drug was administered intraperitoneally to mice at doses of 20 mg/kg/day, beginning on day 0 for 20 days. The control mice received 1% dimethyl sulfoxide (DMSO) simultaneously with HTLV-1-infected cells. In other experiments, Bay 11-7082 or DMSO was also administered into the tumor site directly everyday for 15 days at the same doses as stated above 10 days after tumor formation.

RESULTS

Rapid growth of HTLV-1-infected cell lines inoculated in NOG mice. To investigate the in vivo growth, cells of nine IL-2-independent HTLV-1-infected cell lines were inoculated subcutaneously in the postauricular region of NOG mice (Table 1). Mice inoculated with seven cell lines [ED-40515(−), SLB-1, MT-1, TL-Oml, Hut-120, MT-2, and MT-4] produced a visible tumor within 2 to 3 weeks in NOG mice (Fig. 1). The remaining two transformed cell lines (M8116 and TY8-3/MT-2) failed to form a visible tumor during the 2- to 3-week follow-up period although the mice inoculated with these cell lines were found to have sesame-like tumors at the inoculated site after excision of skin. Histological analysis revealed that the sesame-like tumors consist of small number of nonmitotic cells scattering in the scar tissue. Furthermore, no leukemic infiltration was found in various organs of mice with sesame-like tumors (Table 2). Five cell lines [ED-40515(−), SLB-1, Hut-102, MT-1, and TL-Oml] produced a progressively growing large tumor. Especially, ED-40515(−) leukemic and SLB-1 transformed cell lines were most efficient resulting in the formation of a large tumor in NOG mice only after 2 weeks. It was notable that SLB-1- and Hut-102-transformed cell lines produced a hemorrhagic hard tumor and ED-40515(−), MT-1, and TL-OmI leukemic cell lines produced a soft tumor in NOG mice. The average tumor size in NOG mice inoculated with ED-40515(−) and SLB-1 was 25 by 20 by 12 mm and 19 by 10 by 16 mm, respectively, 2 weeks after inoculation. These results showed that most of the cell lines inoculated subcutaneously into the postauricular region of NOG mice were able to produce a large tumor very efficiently, irrespective of whether they were leukemic or in vitro transformed cells.

Comparison of ED-40515(−) cells growth in NOG and NOD-SCID mice. To assess and clarify the mechanism of in vivo tumor cell growth in NOG mice, we inoculated cells of the ED-40515(−) cell line (10^7 cells) subcutaneously into NOG mice without common γ-chain. For comparison, mice of the parent strain, NOD-SCID with common γ-chain, were also used. Three NOD-SCID and three NOG mice were sacrificed 1 week as well as 2 weeks after inoculation. Results showed that there was significant difference in successful engraftment of tumor cells in an individual mouse of both strains. In the case of NOG mice the number of cells increased from initial level by about 7.6 and 23.6-fold on day 8 and 15, respectively. In control NOD-SCID mice, the number of inoculated cells was decreased by about 4.59- and 2.73-fold on day 8 and 15, respectively (Fig. 2). The common γ-chain is a critical molecule for the development of T and NK cells (6, 13). In addition, a defect of dendritic cell function was reported (13). Thus, these results suggest that NK deficit or functional defects in dendritic cells are responsible for the production of a progressively growing large tumor in NOG mice.

Infiltration of HTLV-1-infected cell lines into the different

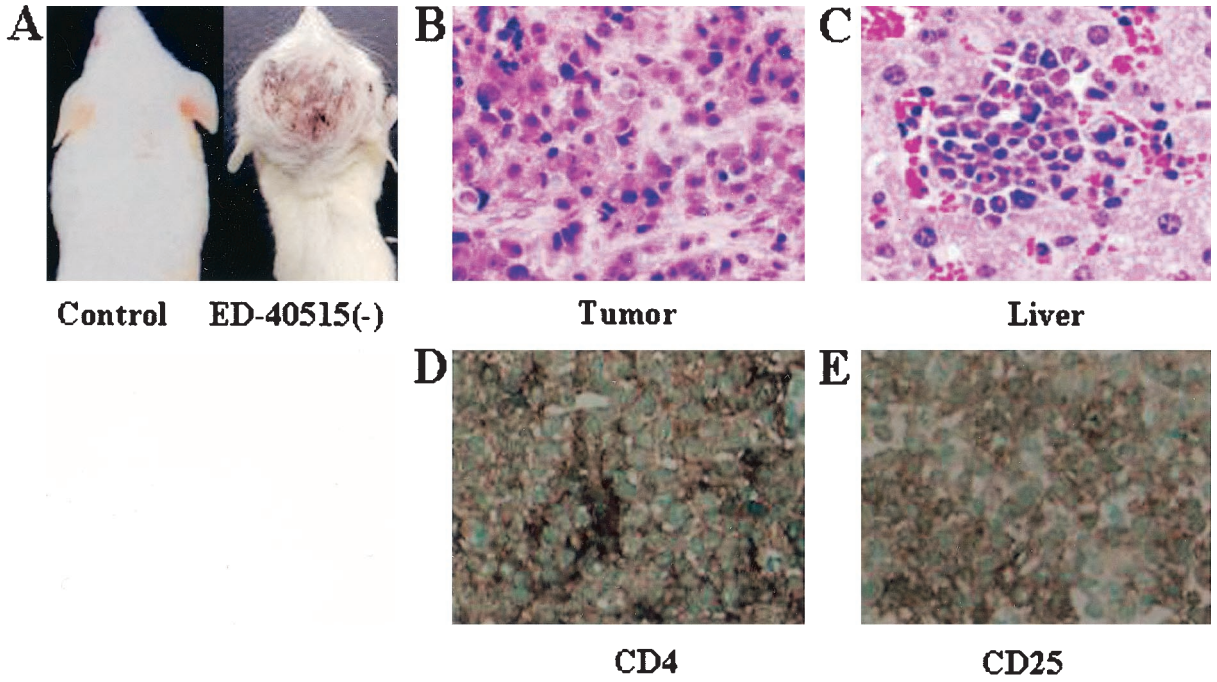

FIG. 1. Tumor growth and infiltration in NOG mice. (A) Photographs of normal NOG mice and those inoculated with ED-40515(−) cells subcutaneously in the postauricular region after 3 weeks. H&E staining of tumor tissue of an ED-40515(−) injected mouse (B) and a section of the tumor-bearing liver of an SLB-1-inoculated mouse (C). In vivo expression of CD4 and CD25 are revealed by immunohistochemistry. Immunohistochemical staining using anti-CD4 (D) and anti-CD25 (E) was conducted on tumor tissues from mice 2 weeks after inoculation of the ED-40515(−) cell line.

organs of NOG mice. To assess the tissue distribution of HTLV-1-infected cell lines, we carried out histological examinations of the different organs of NOG mice inoculated with different types of cell lines (Table 2). Inoculation of HTLV-1-infected cell lines led to progressive tumor formation at the inoculated site and infiltration into peripheral circulation. Proliferation and infiltration of tumor cells were found not only in primary tumor tissues, but also in peripheral blood, bone marrow, lung, liver, spleen and kidney of NOG mice inoculated with the ED-40515(−) cell line. Additionally, the heart and brain were also involved in NOG mice inoculated with the SLB-1 cell line. We also found that mice inoculated with Hut-102, MT-1 and TL-Oml cell lines exhibited infiltration in various organs in a similar manner as that of leukemia, eventually resulting in death. H&E staining showed a massive infiltration of tumor cells at the site of inoculation with ED-40515(−) and in the liver inoculated with the SLB-1 cell line (Fig. 1B and C, respectively). These data suggest that HTLV-1-infected cell lines could invade different organs of SCID mice in a leukemic manner, irrespective of their origin. Interestingly, Tax-positive in vitro transformed cell lines appeared to infiltrate the various organs of mice more aggressively and massively than leukemic cell lines.

Expression of surface proteins in the tumor tissues in mice inoculated with HTLV-1-infected cell lines. To investigate protein expression of T-cell surface antigens by immunohistochemistry, cytospin samples of in vitro culture cells and tissue sections from the tumor of mice inoculated with the

TABLE 2. Infiltration of leukemic cells into different organs of SCID mice[a]

Cell line	Infiltration of leukemic cells into:								
	Tumor	Peripheral blood	Bone marrow	Liver	Spleen	Lung	Brain	Kidney	Heart
ED-40515(−)	+++	++	±	+	+	+	±	+	−
SLB-1	+++	+++	++	+++	++	+++	+	+	+
MT-1	+++	++	−	+	+	+	+	−	−
TL-oml	+++	++	−	+++	+	±	−	−	−
Hut-102	+++	++	+++	+++	+++	+	±	−	−
MT-2	++	+	±	±	+	±	−	+	−
MT-4	++	+	±	−	+	−	−	−	−
M8116	+	±	−	−	−	−	−	−	−
TY8-3/MT-2	+	−	−	−	−	−	−	−	−

[a] Mice were injected with 1×10^7 to 7.5×10^7 cells per mouse. Tumor tissue and organ samples were examined by histological analysis. Symbols: +, slight infiltration; ++, marked infiltration; +++, massive infiltration; ±, slight or no infiltration, depending on each mouse; −, no infiltration.

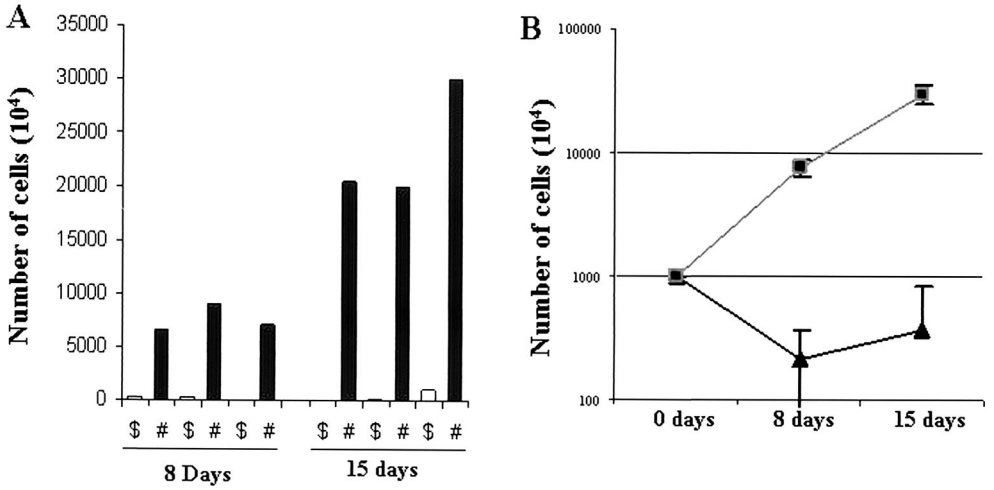

FIG. 2. Comparison of ED-40515(−) cell growth in NOG and NOD-SCID mice. To evaluate the in vivo growth pattern of tumor cells in SCID mice, we inoculated the ED-40515(−) cell line (10^7) in both NOD-SCID and NOG mice. (A) Tumor cells obtained from mice on day 8 and 15 were counted by the trypan blue method. Open and black bars represent the number of cells in individual NOD-SCID ($) and NOG (#) mice, respectively. (B) Mean results ± standard error (error bars) from three mice of individual strains on day 8 and 15 (the squares and triangles represent NOG and NOD-SCID mice, respectively).

ED-40515(−) cell line were examined. In vitro cultured ED-40515(−) and SLB-1 cell lines expressed both human CD4 and CD25 abundantly (data not shown). A higher level of IL-2 receptor α (IL-2Rα) (CD25) expression was observed on the surface of the malignant cells associated with all stages of ATL (41–43). Immunohistochemical staining indicated that in vivo tumor ED-40515(−) cells also expressed human CD4 and CD25 (Fig. 1D and E). In addition, we stained in vitro and in vivo samples to evaluate the protein expression of CD8 and CD3. Both in vitro and in vivo samples showed that tumor cells were positive for CD3, but not CD8 (data not shown). We also examined the expression of HTLV-1 viral antigen Tax and Gag (p19) by immunohistochemical staining and Western blot. Cells of the tumor mass formed after inoculation with SLB-1 cell line were apparently positive for the Tax and Gag antigens, whereas those after inoculation of the ED-40515(−) cell line were negative for the Tax and Gag antigens (Fig. 3A and B). These results indicated that there was no obvious change in

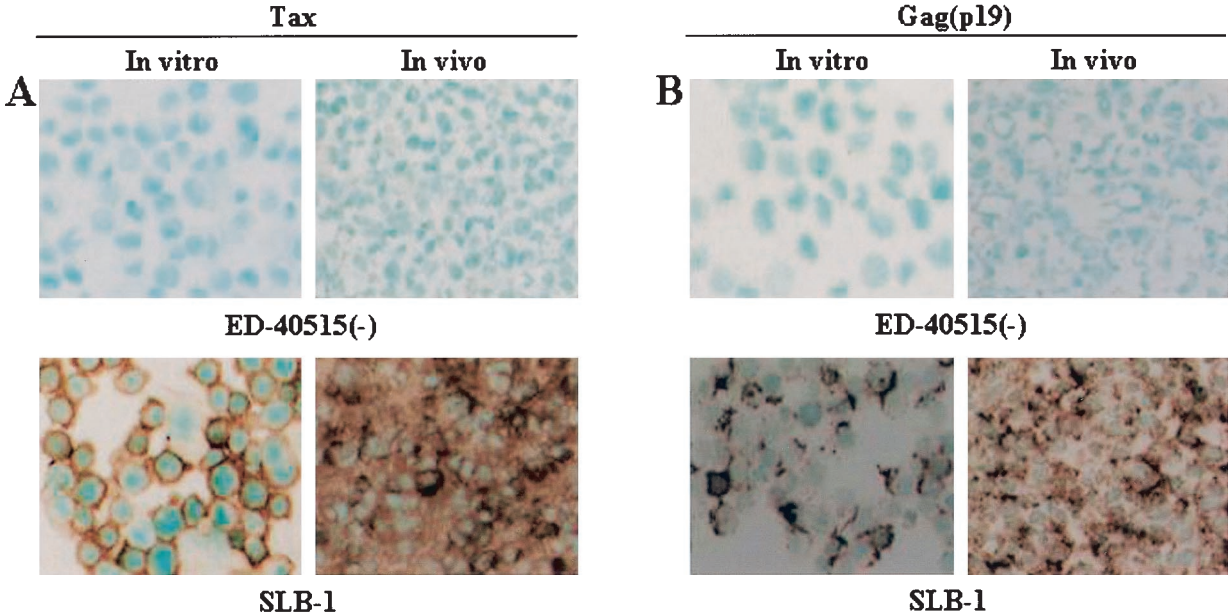

FIG. 3. Viral protein expression in the cell lines inoculated in NOG mice. To investigate viral protein expression in the cell lines inoculated in mice, we performed immunohistochemical analysis. In vitro cytospin sample and in vivo tumor tissue from mice 2 weeks after inoculation with cell lines were stained with anti-Tax (A) and anti-Gag antibody (B). Upper and lower panels of both figures represent the ED-40515(−) and SLB-1 cell lines, and the right and left panels show in vitro and in vivo sample, respectively.

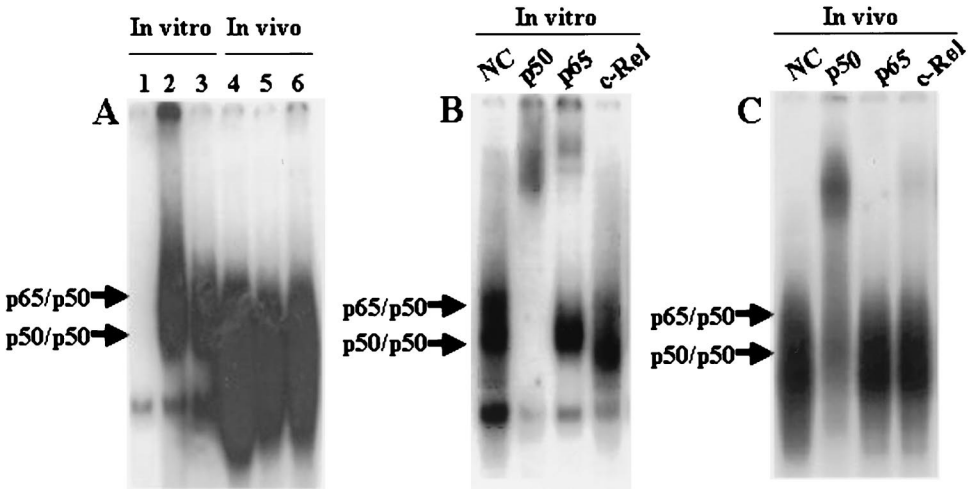

FIG. 4. NF-κB binding activity of ED-40515(−) cells in NOG mice. (A) Analysis of NF-κB binding activity of the ED-40515(−) cell line both in vitro and in vivo by EMSA. Nuclear extracts (5 μg) were treated with ^{32}P-labeled wild-type NF-κB oligonucleotides. Lane 1 contains the negative control using Jurkat, and lane 2 contains the positive control using the SLB-1 cell line. Lane 3 and lanes 4 to 6 show in vitro and in vivo NF-κB DNA binding of ED-40515(−) cells from three different tumor-bearing mice, respectively. (B and C) Analysis of the NF-κB components of ED-40515(−) cells by supershift assay. Supershift using antibodies specific to p50, p65, and c-Rel subunits of NF-κB were conducted both in vitro (B) and in vivo (C). NC, negative control.

protein expression before and after inoculation of HTLV-1-bearing cells in mice.

NF-κB binding activity of ED-40515(−) cells inoculated in NOG mice. High NF-κB binding activity is thought to be crucial for maintaining the characteristics of both ATL/L cells and in vitro transformed cells with HTLV-1. To determine whether or not NF-κB activity is changed in vivo, we performed EMSA. Interestingly, it was shown that in vivo NF-κB DNA binding activity of the tumor cells was even stronger than that of the in vitro sample (Fig. 4A). Furthermore, we investigated whether or not the NF-κB specific bands of tumor tissues originated from the inoculated cells. For this purpose, super-shift assays were performed with nuclear extracts of tumor tissues in the absence or presence of antibodies that specifically recognize the following members of the NF-κB family: p50, p65, and c-Rel. The band was super-shifted by p50 antibody and also by c-Rel antibody, demonstrating that the band contained transactivating p50 and c-Rel (Fig. 4C). This pattern was apparently different from that of in vitro culture cells of ED-40515(−), where the band was super-shifted by p50 and p65 antibodies (Fig. 4B).

Antitumor effect of Bay 11-7082 through the inhibition of NF-κB. To determine the effect of Bay 11-7082 on primary and infiltrative tumor cell growth, we inoculated ED-40515(−) cells (10^7) subcutaneously into the postauricular region of NOG mice. Mice were intraperitoneally administered Bay 11-7082 (20 mg/kg of body weight/day) or 1% DMSO together with the inoculation of tumor cells. There was no significant difference in tumor size in any of the mice of both the Bay and DMSO group 20 days after treatment. However, Bay 11-7082-treated mice appeared to be healthy and had no standing of hair, weight loss and cachexia, all of which are signs of near death. In contrast, the control mice showed these clinical signs of near death. Notably, Bay 11-7082 suppressed infiltration of the tumor cells into peripheral blood and other organs while control mice showed infiltration of the tumor cells in peripheral blood as well as other organs of SCID mice (Fig. 5A and B). Accordingly, these results strongly suggest that leukemic infiltration of the tumor cells may contribute to aggravation of the clinical status of the tumor-bearing mice.

We then tested the effects of Bay 11-7082 on the growth of established subcutaneous ED-40515(−) tumors (Fig. 5C and D). Ten days after tumor formation, Bay 11-7082 (20 mg/kg/day) was administered directly into the tumor site daily whereas control mice received 1% DMSO for 15 days. The tumor rapidly grew in control mice, resulting in the development of death signs due to disease progression in all mice. In contrast, the tumors began to regress markedly and later, widespread tumor necrosis occurred in Bay 11-7082-treated mice (Fig. 5C). These data indicate that Bay 11-7082 significantly inhibited the growth of an established tumor.

Collectively, these results suggest that daily administration of Bay 11-7082 could prevent primary tumor growth and disease progression through the inhibition of infiltrative leukemic cell growth in various organs.

DISCUSSION

ATL is a malignancy of T-lymphocytes etiologically linked to a retrovirus, human T-cell leukemia virus type 1 (HTLV-1) (33, 48). Previous results showed that HTLV-1-infected transformed cell lines do not have sufficient activity to acquire tumorigenic potential in SCID mice, but leukemic cell lines do produce a tumor during a 2- to 4-month follow-up period (10, 16). In the present study using a novel SCID mouse, NOG, successful engraftment of both transformed and leukemic cells was achieved during a 2- to 3-week follow-up period, producing a progressively growing large tumor. This extremely rapid tumor formation is one of the hallmarks of our animal model. Very recently, Liu et al. demonstrated that the efficiency of tumorigenesis by HTLV-1-transformed cell lines is dramatically elevated in NOD-SCID mice when mice are sublethally

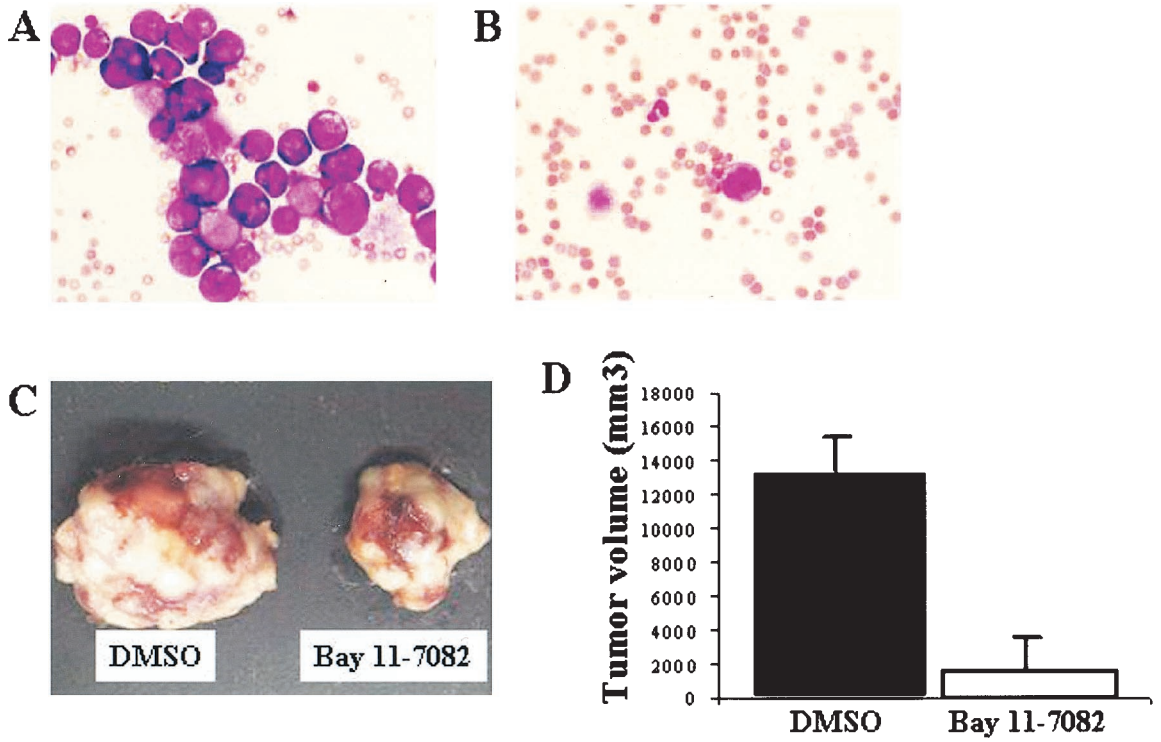

FIG. 5. Effect of Bay 11-7082 on primary and infiltrative tumor cell growth. Mice were injected subcutaneously via the postauricular region with ED-40515(−) cells (10^7). At the same time, either 1% DMSO or Bay 11-7082 (20 mg/kg/day) was administered intraperitoneally to the mice every day for 20 days. Another group of experiments were conducted using administration of the same doses of DMSO or Bay 11-7082 at the tumor site 10 days after tumor formation for 15 days. May-Grunwald and Giemsa staining showed infiltration of tumor cells in PBMNCs of mice treated with DMSO (A) or Bay 11-7082 (B) after 3 weeks, respectively. Photographs of subcutaneously formed ED-40515(−) tumors (C) and tumor volume (D) in the mice that had received DMSO or Bay 11-7082 10 days after tumor formation at the tumor site. Black bars represent the DMSO-treated control mice, and open bars represent the Bay 11-7082-treated mice. Each result was obtained from three different mice (means are shown [error bars, standard errors]).

irradiated prior to inoculation (25). Interestingly, it was shown that transformed cell lines produced a hemorrhagic hard tumor and leukemic cell lines produced a soft tumor in NOG mice. The hemorrhagic tumor could be explained by the augmented invasiveness to blood vessels. Further study is needed to determine whether or not this was due to the effect of Tax expressed in transformed cell lines such as SLB-1 and Hut-102.

Infiltrations of HTLV-1-infected leukemic cell lines into various organs are well known in ATL patients (38, 45). We found that SCID mice inoculated with ED-40515(−) cells showed infiltration into peripheral blood, bone marrow, lung, liver, spleen and kidney, and in addition to these organs, cells of the SLB-1 cell line had also infiltrated into the brain and heart (Table 2). These results indicate that HTLV-1-bearing cells in our model could infiltrate in a similar manner as leukemic cells in ATL patients. Leukemic infiltration was more remarkable in Tax-positive transformed cell lines than in leukemic cell lines. Further study is necessary to elucidate whether or not the expression of Tax in transformed cell lines is responsible for this role.

The differing behaviors of HTLV-1-infected cell lines in different types of SCID mice in the formation of tumors are dependent on the host immune system. Natural killer cells in the mice might play an important role in the rejection of implanted tissues or cells in SCID mice (5, 8, 10, 11, 37, 46, 47). In addition, recipient dendritic cells could have a role in transplant rejection (24). In this study, we compared two strains of NOG and NOD-SCID mice to directly assess in vivo HTLV-1-infected cell growth. In addition to the absence of T and B cells, NOG mice have no NK and there are also functional defects in dendritic cells (18). Our data showed that the number of ED-40515(−) cells inoculated in NOG mice was significantly increased about 7.6- and 23.6-fold, whereas the mass of tumor cells inoculated in NOD-SCID mice was reduced about 4.59- and 2.73-fold after 1 and 2 weeks, respectively (Fig. 2). In the present study, HTLV-1-infected cell lines inoculated subcutaneously in the postauricular region over the skeleton of mice permitted us to quickly observe the tumor growth macroscopically and to measure the size of the tumor. By measuring the size of the tumor macroscopically, it was possible to easily compare growth ability between the control mice and mice inoculated with the ED-40515(−) cell line (Fig. 1A). The present animal and inoculation system are applicable to other malignant cells and cell lines of different origins that are unrelated to HTLV-1 (unpublished results), and therefore could be very useful in the study of tumorigenesis of various malignant tissues in general.

Tax is a 40-kDa nuclear oncoprotein, which is responsible for trans-activation of the HTLV-1 long terminal repeat (9, 36), as well as numerous cellular genes involved in T-cell ac-

tivation and growth, such as those encoding IL-2 (26), and the α-chain of IL-2R (CD25, Tac) (3, 7). The malignant cells associated with all phases of ATL express very high levels of IL-2Rα (41–43)without expressing a significant amount of Tax. Our results showed that tumor tissues in NOG mice also expressed both IL-2Rα and T-cell surface molecule CD4 as assessed by the immunohistochemical procedure used in this study, and these levels were reminiscent of those seen in primary ATL cells (Fig. 1D and E).

Many cellular genes are shown to be activating through stimulation of the NF-κB/Rel family of transcription factors when Tax is expressed in the cells. The inactivation of tumor suppressor p53 by Tax in HTLV-1-positive cells is also dependent on activation of the NF-κB pathway (32). Leukemic cells in the ATL patients and leukemic cell lines directly originating from the patients apparently share this character with Tax-expressing cells in the absence of Tax. For this reason, NF-κB, rather than Tax, is considered to play a key role in the pathogenesis of HTLV-1-associated malignancy (15). Recent studies have provided some insights into the multiple aspects of NF-κB involvement in oncogenesis, including the control of apoptosis, the cell cycle, differentiation and migration of the cells (2). In this study, we inoculated a Tax nonexpressing ED-40515(−) cell line in NOG mice to evaluate the role of NF-κB binding activities and Tax expression in tumor cells. As a result, the ED-40515(−) cell line inoculated into SCID mice did not express Tax (data not shown). It was shown that in vivo NF-κB DNA binding activity of the tumor cells was even stronger than those cultured in vitro (Fig. 4A). Moreover, although the NF-κB components of ED-40515(−) cells grown in vitro were p50 and p65 (Fig. 4B), those in tumor cells consisted of p50 and c-Rel (Fig. 2). Such quantitative as well as qualitative alterations in NF-κB activity and the NF-κB components seen in tumor cells in vivo might play an important role in the development of rapid growth of tumors in SCID mice. This NOG mice model we present here would be useful in identifying such in vivo changes of the cells. Further study is necessary to clarify the mechanism underlying the rapid growth of the tumor and in vivo change of NF-κB components.

To develop potential new therapeutic strategies for ATL, Bay 11-7082 was used for the in vivo experiment. Very recently, we showed that Bay 11-7082 induced apoptosis in HTLV-1-infected cell lines and primary ATL cells, whereas the effect against HTLV-1-negative cells was only negligible (29). Bay 11-7082 rapidly and specifically reduced DNA binding of NF-κB in HTLV-1-infected T-cell lines, and down-regulated expression of the antiapoptotic gene, Bcl-XL. Due to its potent and selective inhibition of phosphorylation of IκBα, we predicted that Bay 11-7082 would be useful in the treatment of ATL. Our results clearly indicate that exclusive use of Bay 11-7082 could significantly prevent tumor growth at the inoculated site and infiltrative leukemic cell growth in SCID mice through inhibition of NF-κB activity (Fig. 5). In our NOG mice model, Bay 11-7082 showed no significant and severe adverse effect against the mice during the treatment period. These data strongly suggest that NF-κB might serve as a general therapeutic target of ATL and Bay 11-7082 could be used as a lead compound in the development of anti-ATL drugs.

In summary, our NOG mice model system provides the opportunity to understand and investigate the mechanism of pathogenesis and malignant cell growth of ATL and to develop a novel therapeutic regimen.

ACKNOWLEDGMENTS

We thank S. Yamaoka, S. Horiuchi, N. Yamamoto, N. Begum, N. Chinanonwait, and N. Saito for their advice and assistance with the experiments. We also thank Y. Sato of the National Institute of Infectious Diseases for excellent technical assistance.

This work was supported by grants from the Ministry of Education, Science, and Culture and the Ministry of Health, Labor, and Welfare of Japan.

REFERENCES

1. **Adams, J., V. J. Palombella, and P. J. Elliott.** 2000. Proteasome inhibition: a new strategy in cancer treatment. Investig. New Drugs **18:**109–121.
2. **Baldwin, A. S.** 1999. The NF-κB and IκB proteins: new discoveries and insights. Annu. Rev. Immunol. **14:**649–681.
3. **Ballard, D. W., E. Bohnlein, J. W. Lowenthal, Y. Wano, B. R. Franza, and W. C. Greene.** 1988. HTLV-1 tax induces cellular proteins that activate the κB element in the IL-2Rα gene. Science **241:**1652–1655.
4. **Bosma, G. C., R. P. Custer, M. J. Bosma.** 1983. A severe combined immunodeficiency mutation in the mouse. Nature **301:**527–530.
5. **Bukowshi, J. F., J. F. Wamer, G. Dennert, and R. M. Welsh.** 1985. Adoptive transfer studies demonstrating the antiviral effect of natural killer cells in vivo. J. Exp. Med. **161:**40–52.
6. **Cao, X., E. W. Shores, L. J. Hu, M. R. Anver, B. L. Kelsall, S. M. Russell, J. Dargo, M. Noguchi, A. Grinberg, E. T. Bloom, W. E. Paul, S. I. Katz, P. E. Love, and W. J. Leonard.** 1995. Defective lymphoid development in mice lacking expression of the common cytokine receptor gamma chain. Immunity **2:**223–238.
7. **Cross, S. L., M. B. Feinberg, N. Holbrook, F. Wong-Staal, and W. J. Leonard.** 1987. Regulation of human interleukin-2 receptor alpha chain promoter: Activation of a nonfunctional promoter by the transactivator gene of HTLV-1. Cell **49:**47–56.
8. **Dorshkind, K., S. B. Pollack, M. J. Bosma, andR. A. Phillips.** 1985. Natural killer (NK) cells present in mice with severe combined immunodeficiency (scid). J. Immunol. **134:**3798–3801.
9. **Felber, B. K., H. Paskalis, C. Kleinman-Ewing, F. Wong-Staal, and G. N. Pavlakis.** 1985. The pX protein of HTLV-1 is a transcriptional activator of its long terminal repeats. Science **229:**675–679.
10. **Feuer, G., S. A. Stewart, S. M. Baird, F. Lee, R. Feuer, and I. S. Y. Chen.** 1994. Potential role of natural killer cells in controlling tumorigenesis by human T-cell leukemia Viruses. J. Virol. **69:**1328–1333.
11. **Garni-Wagner, B. A., P. L. Witte, M. M. Tutt, W. A. Kuziel, P. W. Tucker, M. Bennett, and V. Kumar.** 1990. Natural killer cells in thymus: studies in mice with severe combined immune deficiency. J. Immunol. **144:**796–803.
12. **Gassain, A., F. Brain, and J. C. Vernant.** 1985. Antibodies to human T-lymphotropic virus type 1 in patients with tropical spastic paraparesis. Lancet **ii:**407–410.
13. **Goldman, J. P., M. P. Blundell, L. Lopes, C. Kinnon, J. P. Di Santo, and A. J. Thrasher.** 1998. Enhanced human cell engraftment in mice in RAG2 and the common cytokine receptor gamma chain. Br. J. Haematol. **103:**335–342.
14. **Hideshima, T., D. Chauhan, P. Richardson, C. Mitsiades, N. Mitsiades, T. Hayashi, N. Munshi, L. Dong, A. Castro, V. Palombella, J. Adams, and K. C. Anderson.** 2002. NF-κB as a therapeutic target in multiple myeloma. J. Biol. Chem. **277:**16639–16647.
15. **Hiscott, J., H. Kwon, and P. Genin.** 2001. Hostile takeover: viral appropriation of the NF-κB pathway. J. Clin. Investig. **107:**143–151.
16. **Imada, K., A. Takaori-Kondo, T. Akagi, K. Shimotohno, K. Sugamura, T. Hattori, H. Yamabe, M. Okuma, and T. Uchiyama.** 1995. Tumorigenicity of human T-cell leukemia virus type I infected cell lines in severe combined immunodeficient mice and characterization of the cells proliferating in vivo. Blood **86:**2350–2357.
17. **Ishihara, S., N. Tachibana, A. Okayama, K. Murai, K. Tsuda, and N. Mueller.** 1992. Successful graft of HTLV-I-transformed human T-cells (MT-2) in severe combined immunodeficiency mice treated with anti-asialo GM-1 antibody. Jpn. J. Cancer Res. **83:**320–323.
18. **Ito, M., H. Hiramatsu, K. Kobayashi, K. Suzue, M. Kawahata, K. Hioki, Y. Ueyama, Y. Koyanagi, K. Sugamura, K. Tsuji, T. Heike, and T. Nakahata.** 2002. NOD/SCID/γc^{null} mouse: An excellent recipient mouse model for engraftment of human cells. Blood **100:**3175–3182.
19. **Izban, K. F., M. Ergin, J-Z. Qin, R. L. Martinez, R. J. Pooley, J. R., S. Saeed, and S. Alkan.** 2000. Constitutive expression of NF-κB is a characteristic feature of mycosis fungoides: Implication for apoptosis resistance and pathogenesis. Hum. Pathol. **31:**1482–1490.
20. **Kamel-Reid, S., M, Letarte, M. Doedens, A. Greaves, B. Murdoch, T. Grunberger, Lapidot, T. Lapidot, P. Thorner, M. H. Freedman, R. A. Philips, and J. E. Dick.** 1991. Bone marrow from children in relapse with pre-B acute lymphoblastic leukemia proliferates and disseminates rapidly in scid mice. Blood **78:**2973–2981.

21. **Kamel-Reid, S., M. Letarte, C. Sirard, M. Doedens, T. Grunberger, G. Fulop, M. H. Freedman, R. A. Philips, and J. E. Dick.** 1989. A model of lymphoblastic leukemia in immune-deficient SCID mice. Science **246:**1597–1600.
22. **Keller, S. A., E. J. Schattner, and E. Cesarman.** 2000. Inhibition of NF-κB induces apoptosis of KSHV-infected primary effusion lymphoma cells. Blood **96:**2537–2542.

22a. **Kieran, M., V. Blank, F. Logeat, J. Vandekerckhove, F. Lottspeich, O. Le Bail, M. B. URban, P. Kourilsky, P. A. Baeuerle, and A. Israel.** 1990. The DNA binding subunit of NF-kappa B is identical to factor KBF1 and homologous to the rel oncogene product. Cell **62:**1007–1018.

23. **Kitajima, I., T. Shinohara, J. Bilakovics, D. A. Brown, X. Xu, and M. Nerenberg.** 1992. Ablation of transplanted HTLV-1 Tax transformed Tumors in mice by antisense inhibition of NF-κB. Science **258:**1792–1795.
24. **Lechler, R., W. F. Ng, and R. M. Steinman.** 2001. Dendritic cells in transplantation—friends or foe? Immunity **14:**357–368.
25. **Liu, Y., K. Dole, J. R. L. Stanley, V. Richard, T. J. Rosol, L. Ratner, M. Lairmore, G. Feuer.** 2002. Engraftment and tumorigenesis of HTLV-1 transformed T cells in SCID/bg and NOD-SCID mice. Leukemia Res. **26:**561–567.
26. **Maruyama, M., H. Shibuya, H. Harada, M. Hatakeyama, M. Seiki, T. Fujita, J. Inoue, M. Yoshida, and T. Taniguchi.** 1987. Evidence for aberrant activation of the interleukin-2 autocrine loop by HTLV-1 encoded p40^{x} and T3/Ti complex triggering. Cell **48:**343–350.
27. **McCune, J. M., R. Namikawa, H. Kaneshima, L. D. Scultz, M. Lieberman, and I. L. Weissman.** 1988. The SCID-hu mouse: Murine model for the analysis of human hematolymphoid differentiation and function. Science **241:**1632–1639.
28. **Mori, N., M. Fujii, S. Ikeda, Y. Yamada, M. Tomonaga, D. W. Ballard, and N. Yamamoto.** 1997. Constitutive activation of NF-κB in primary adult T-cell leukemia cells. Blood **93:**2360–2368.
29. **Mori, N., Y. Yamada, S. Ikeda, Y. Yamasaki, K. Tsukasaki, Y. Tanaka, M. Tomonaga, N. Yamamoto, and M. Fujii.** 2002. Bay 11–7082 inhibits transcription factor NF-κB and induces apoptosis of HTLV-1-infected T-cell lines and primary adult T-cell leukemia cells. Blood **100:**1828–1834.
30. **Mosier, D. E.** 1991. Adoptive transfer of human lymphoid cells to severely immunodeficient mice: Models for normal human immune function, autoimmunity, and AIDS. Adv. Immunol. **50:**303–325.
31. **Pierce, J. W., R. Schoenleber, G. Jesmok, J. Best, S. A. Moore, T. Collins, and M. E. Gerritsen.** 1997. Novel inhibitors of cytokine-induced IκBα phosphorylation and endothelial cell adesion molecule expression show anti-inflammatory effects in vivo. J. Biol. Chem. **272:**21096–21103.
32. **Pise-Masision, C. A., R. Mahieux, H. Jiang, M. Ascroft, M. Radonovich, J. Duvall, C. Guillerm, and J. N. Brady.** 2000. Inactivation of p53 by human T-cell lymphotrophic virus type I Tax requires activation of the NF-κB pathway and is dependent on p53 phosphorylation. Mol. Cell. Biol. **20:**3377–3386.
33. **Poiesz, B. J., F. W. Ruscetti, A. F. Gazdar, P. A. Bunn, J. D. Minna, and R. C. Gallo.** 1980. Detection and isolation of type C retrovirus particles from fresh and cultured lymphocytes of a patient with cutaneous T-cell lymphoma. Proc. Natl. Acad. Sci. USA **77:**7415–7419.
34. **Sawyers, C. L., M. L. Gishizky, S. Quan, D. W. Golde, and O. N. Witte.** 1992. Propagation of human blastic myeloid leukemias in the SCID mouse. Blood **79:**2089–2098.
35. **Schmidt-Wolf, I. G. H., R. S. Negrin, H. Kiem, K. G. Blume, and I. L. Weissman.** 1991. Use of SCID mice/human lymphoma model to evaluate cytokine-induced killer cells with potent antitumor cell activity. J. Exp. Med. **174:**139–149.
36. **Sodroski, J. G., C. A. Rosen, and W. A. Haseltine.** 1984. Trans-acting transcriptional activation of the long terminal repeat of human T lymphotropic viruses in infected cells. Science **225:**381–385.
37. **Storkus, W. J., R. D. Salter, J. Alexander, F. E. Ward, R. E. Ruiz, P. Cresswell, and J. R. Dawson.** 1991. Class I-induced resistance to natural killing: Identification of nonpermissive residues in HLA-A2. Proc. Natl. Acad. Sci. USA **88:**5989–5992.
38. **Tamura, K.** 1996. Clinical classification of adult T-cell leukemia and its complications. Rinsho Byori **44:**19–23.
39. **Tan, C., and T. A. Waldmann.** 2002. Proteasome inhibitor PS-341, a potential therapeutic agent for adult T-cell leukemia. Cancer Res. **62:**1083–1086.
40. **Teicher, B. A., G. Ara, R. Herbst, V. J. Palombella, and J. Adams.** 1999. The proteasome inhibitor PS-341 in cancer therapy. Clin. Cancer Res. **5:**2638–2645.
41. **Uchiyama, T., S. Brober, and T. A. Waldmann.** 1981. A monoclonal antibody (anti-Tac) reactive with activated and functionally mature T-cells. I. Production of anti-Tac monoclonal antibody and distribution of Tac (+) cells. J. Immunol. **126:**1393–1397.
42. **Uchiyama, T., T. Hori, M. Tsudo, Y. Wano, H. Umadome, S. Tamori, J. Yodoi, M. Maeda, and H. Uchino.** 1985. Interleukin-2 receptor (Tac antigen) expressed on adult T-cell leukemia cells. J. Clin. Investig. **76:**446–453.
43. **Waldmann, T. A., W. C. Greene, P. S. Sarin, C. Saxinger, D. W. Blayney, W. A. Blattner, C. K. Goldman, K. Bongiovanni, S. Sharrow, J. M. Depper, W. Leonard, T. Uchiyama, and R. C. Gallo.** 1984. Functional and phenotypic comparison of human T-cell leukemia and lymphoma virus positive adult T-cell leukemia with human T-cell leukemia virus negative Sezary leukemia, and their distinction using anti-Tac monoclonal antibody identifying the human receptor for T-cell growth factor. J. Clin. Investig. **73:**1711–1718.
44. **Waller, E. K., O. W. Kamel, M. L. Cleary, A. S. Majumdar, M. R. Schick, M. Lieberman, and I. L. Weissman.** 1991. Growth of primary T-cell non-Hodgkin's lymphomata in SCID-hu mice: requirement of a human lymphoid microenvironment. Blood **78:**2650–2665.
45. **Watanabe, T.** 1997. HTLV-I-associated diseases. Int. J. Hematol. **66:**257–278.
46. **Welsh, R. M.** 1986. Regulation of virus infections by natural killer cells: a review. Nat. Immun. Cell Growth Regul. **5:**169–199.
47. **Welsh, R. M., J. O. Brubaker, M. Vargas-Cortes, and C. L. O'Donnell.** 1991. Natural killer (NK) cell response to virus infections in mice with severe combined immunodeficiency. The stimulation of NK cells and the NK cell-dependent control of virus infections occur independently of T and B cell function. J. Exp. Med. **173:**1053–1063.
48. **Yoshida, M., I. Miyoshi, Y. Hinuma.** 1982. Isolation and characterization of retrovirus from cell lines of human adult T-cell leukemia and its implication in the disease. Proc. Natl. Acad. Sci. USA **79:**2031–2035.